

Design of IIR multiple-notch filters with symmetric magnitude responses about notch frequencies

Ivan Krstić · Saša Nikolić · Goran Stančić ·
Predrag Lekić

Received: date / Accepted: date

Abstract A novel all-pass based infinite impulse response (IIR) digital multiple-notch filter design method is presented in this paper. The proposed method ensures that, for an arbitrary pass-bands ripple value, specifications regarding positions of notch, left- and right-hand cutoff frequencies are exactly met, which leads to symmetric magnitude responses about notch frequencies. Although iterative in its nature, proposed method requires a small number of iterations to find coefficients of the multiple-notch filter, making it very useful for designers. Since the magnitude response of the all-pass based IIR multiple-notch filter is more sensitive in the stop-bands than in the pass-bands, sensitivity analysis along with simulation in limited word-length environment is performed.

Keywords digital multiple-notch filter · digital all-pass filter · symmetric magnitude response · least-square solution · worst-case sensitivity

1 Introduction

Digital multiple-notch filters are widely used in various applications [1–3] where there exists the necessity to suppress certain frequency components from a signal

I. Krstić(✉)

University of Priština, Faculty of Technical Sciences, Knjaza Miloša 7, 38220 Kosovska Mitrovica, Serbia
E-mail: ivan.krstic@pr.ac.rs

S. Nikolić

University of Niš, Faculty of Electronic Engineering, Aleksandra Medvedeva 14, 18000 Niš, Serbia
E-mail: sasa.nikolic@elfak.ni.ac.rs

G. Stančić

University of Niš, Faculty of Electronic Engineering, Aleksandra Medvedeva 14, 18000 Niš, Serbia
E-mail: goran.stancic@elfak.ni.ac.rs

P. Lekić

University of Priština, Faculty of Technical Sciences, Knjaza Miloša 7, 38220 Kosovska Mitrovica, Serbia
E-mail: predrag.lekic@pr.ac.rs

spectrum simultaneously while keeping other spectral components intact. In general, multiple-notch filters can be designed either as FIR (finite impulse response) or IIR. Despite the fact that FIR multiple-notch filters are inherently stable and can be easily designed to have linear phase characteristic, narrower stopband widths (higher Q factor) can be achieved with IIR multiple-notch filters having a rather small order.

There are several different approaches to the IIR multiple-notch filter design [4–14]. Design based on a cascade connection of several second-order IIR single notch filters inevitably leads to uncontrollable pass-band gains [6,7]. On the other side, design methods based on the utilization of convex [8,9,12] or genetic algorithm (GA) [13,14] optimization techniques are highly complex, particularly for a greater number of notch frequencies. All-pass based IIR multiple-notch filter design methods were first introduced in [4,5]. After transforming magnitude response specifications of the multiple-notch filter to those of the phase response of an equivalent all-pass filter, a system of linear equations is constructed in order to determine the coefficients of the all-pass filter. Generalization of non-iterative all-pass based IIR multiple-notch filter design methods is given in [6].

While methods [8,10,11] does not take into account specified notch bandwidths, methods given in [4–7,13] consider notch bandwidths specified at attenuation of 3-dB. Either way, final bandwidths, in general, differ from the desired ones. In other words, all specifications can not be exactly met by utilizing these methods. If final bandwidths are narrower than specified ones, transient response to sinusoidal interferences will be longer, while wider bandwidths will lead to a distortion of frequency components close to notch frequencies [15,16]. Only a few of these design methods can be generalized to a case of an arbitrary attenuation value (i.e. pass-bands ripple value) at cutoff frequencies, whereby it is worth to mention that *Method 1* given in [6] is the same method presented in [4,5] with overcome limitations regarding to tangent operations.

The order of the all-pass filter characterizing the desired multiple-notch filter, obtained by the utilization of fore-mentioned all-pass based design methods, is equal to double the number of notch frequencies. The magnitude response of such a multiple-notch filter is equal to absolute value of the cosine of half the phase response of corresponding all-pass filter, which is monotonically decreasing function. Due to this fact, obtained magnitude response in pass-bands has its minimum at cutoff frequencies. Moreover, this fact provides the non-iterative nature of these methods, but all specifications can not be met. If the multiple-notch filter is desired to meet all specifications, the order of the all-pass filter needs to be increased, which leads to a non-monotonic behavior of the cosine function argument, i.e. the magnitude response in pass-bands does not necessarily have its minimal value at cutoff frequencies. The IIR multiple-notch filter design method proposed in this paper, although all-pass based, is iterative in its nature. Obtained filter exactly meets desired specifications. This improvement, as stated, has to come with a price of an increase in the order of the all-pass filter.

Once multiple-notch filter coefficients are determined, it can be realized using one of several equivalent filter structures having different complexity and number of elements. When choosing realization structure, the lowest sensitive one to coefficients quantization errors should be selected. Since the transfer function of the multiple-notch filter is highly sensitive to coefficients quantization errors, due to the

existence of poles lying close to the unit circle, its realization structure should be considered with a great concern. Realization of the multiple-notch filter, using parallel connection of a delay line and an all-pass filter, considered in this paper, exhibits very low sensitivity in pass-bands. It is well known that sensitivity of the all-pass filter phase response to coefficients quantization errors can be considerably reduced if it is realized by cascading first- and second-order all-pass sections, whose realization structures strongly depends on corresponding poles locations [17–21].

The rest of the paper is structured as follows. In Sec. 2, magnitude response specifications of the multiple-notch are transformed to those of the phase response of the equivalent all-pass filter. Nonlinear trigonometric relation between coefficients and phase response of the all-pass filter is also discussed. Sec. 3 contains a detailed explanation of the proposed iterative IIR multiple-notch filter design method, while sensitivity considerations are given in Sec. 4. Design examples are considered in Sec. 5, while a comparison of the proposed to existing all-pass based design methods that can be generalized to a case of an arbitrary pass-bands ripple value, is presented in Sec. 6. Finally, concluding remarks are given in Sec. 7.

2 Problem formulation

This paper deals with the design of IIR multiple-notch filter with K notch frequencies, whose transfer function is assumed to be given by:

$$H(z) = \frac{1}{2} \left[z^{-(N-2K)} + Q_N(z) \right] \quad (1)$$

where $Q_N(z)$ is a transfer function of a stable all-pass filter of N -th order:

$$Q_N(z) = z^{-N} \left(1 + \sum_{i=1}^N q_i z^i \right) \left(1 + \sum_{i=1}^N q_i z^{-i} \right)^{-1} \quad (2)$$

The frequency response of the multiple-notch filter can be obtained by substituting $z = \exp(j\omega)$ in (1), followed by simple mathematical manipulations:

$$H(\exp(j\omega)) = \exp \{ j [\varphi_Q(\omega) - (N - K)\omega] \} \cdot \cos [\varphi_Q(\omega) - K\omega] \quad (3)$$

where:

$$\varphi_Q(\omega) = \frac{\phi_Q(\omega) + N\omega}{2} \quad (4)$$

and $\phi_Q(\omega)$ is a phase response of the all-pass filter $Q_N(z)$.

Since, from equation (3), magnitude response of the multiple-notch filter can be expressed as:

$$\left| H(\exp(j\omega)) \right| = \left| \cos [\varphi_Q(\omega) - K\omega] \right|, \quad (5)$$

the multiple-notch filter's magnitude response approximation problem can be formulated as all-pass filter's phase response approximation problem, i.e. approximation problem of the function $\varphi_Q(\omega)$. Having in mind that the phase characteristic (response) $\phi_Q(\omega)$ of a stable IIR all-pass filter $Q_N(z)$ is monotonically decreasing in

the closed interval $\omega \in [0, \pi]$ and $\phi_Q(0) = 0$, $\phi_Q(\pi) = -N\pi$, the magnitude response given by (5) will have near-one value in i -th pass-band, if $\phi_Q(\omega) - K\omega \approx -(i-1)\pi$, for $i = 1, \dots, K+1$. On the other side, zero values of the magnitude response at notch frequencies $\omega_{n,i}$ will be obtained if $\phi_Q(\omega_{n,i}) - K\omega_{n,i} = -(2i-1)\pi/2$, for $i = 1, \dots, K$.

2.1 Specifications of the multiple-notch filter

Multiple-notch filter specifications are given in the frequency domain and comprise notch frequencies positions ($\omega_{n,i}$), notch bandwidths (BW_i) and pass-bands ripple value (a), for $i = 1, 2, \dots, K$. Left- and right-hand cutoff frequencies are related to notch bandwidths as $\omega_{l,i} = \omega_{n,i} - BW_i/2$ and $\omega_{r,i} = \omega_{n,i} + BW_i/2$, $i = 1, 2, \dots, K$, respectively.

Based on the previous discussion, all-pass filter $Q_N(z)$ design constraints can be formulated as:

$$\phi_Q(\omega_{n,i}) - K\omega_{n,i} = -(2i-1)\pi/2 \quad (6)$$

$$|\phi_Q(\omega) - K\omega + (i-1)\pi| \leq \varepsilon = \arccos 10^{-a/20}, \quad \omega \in \mathcal{P}_i \quad (7)$$

for $i = 1, 2, \dots, K+1$, while i -th pass-band \mathcal{P}_i is defined by:

$$\begin{aligned} \mathcal{P}_1 &= \{\omega \mid 0 \leq \omega \leq \omega_{l,1}\}, \quad \mathcal{P}_{K+1} = \{\omega \mid \omega_{r,K} \leq \omega \leq \pi\} \\ \mathcal{P}_i &= \{\omega \mid \omega_{r,i-1} \leq \omega \leq \omega_{l,i}\}, \quad i = 2, \dots, K \end{aligned} \quad (8)$$

It can be shown easily that if $\phi_Q(\omega) - K\omega$ is monotonically decreasing in the closed interval $\omega \in [0, \pi]$ and if specifications are exactly met at cutoff frequencies:

$$\begin{aligned} \phi_Q(\omega_{l,i}) - K\omega_{l,i} + (i-1)\pi &= -\varepsilon \\ \phi_Q(\omega_{r,i}) - K\omega_{r,i} + i\pi &= \varepsilon \end{aligned} \quad (9)$$

where $i = 1, \dots, K$, then constraints in pass-bands given by (7) are also fulfilled. This is always the case for $N = 2K$, since $\phi_Q(\omega) - K\omega$ becomes equal to $\phi_Q(\omega)/2$, which is monotonically decreasing function. However, this statement is not necessarily true for $N > 2K$.

Equations (6) and (9) suggest that if the all-pass filter $Q_N(z)$ is such that the corresponding $\phi_Q(\omega)$, defined by (4), passes through fixed $3K$ pairs $(\bar{\omega}_m, \phi_Q(\bar{\omega}_m))$, whose positions are independent of the all-pass filter degree:

$$(\bar{\omega}_m, \phi_Q(\bar{\omega}_m)) = \begin{cases} (\omega_{l, \lceil m/3 \rceil}, K\omega_{l, \lceil m/3 \rceil} - \lfloor m/3 \rfloor \pi - \varepsilon), & \langle m \rangle_3 = 1 \\ (\omega_{n, \lceil m/3 \rceil}, K\omega_{n, \lceil m/3 \rceil} - (\lfloor m/3 \rfloor + 0.5)\pi), & \langle m \rangle_3 = 2 \\ (\omega_{r, \lfloor m/3 \rfloor}, K\omega_{r, \lfloor m/3 \rfloor} - \lfloor m/3 \rfloor \pi + \varepsilon), & \langle m \rangle_3 = 0 \end{cases} \quad (10)$$

where $m = 1, 2, \dots, 3K$, and $\langle m \rangle_3$ is the remainder when m is divided by 3, then desired specifications regarding positions of notch, left- and right-hand cutoff frequencies will be exactly met. On the other side, this does not imply that specifications given by (7) are met.

Graphical interpretation of specifications defined by (7) and (10) is given in Fig. 1a), while Fig. 1b) provides an insight of equivalent multiple-notch filter magnitude response specifications. Specifications given by (10) are represented as black dots, while regions defined by (7) are shaded. If $\varphi_Q(\omega)$ is such that it passes through

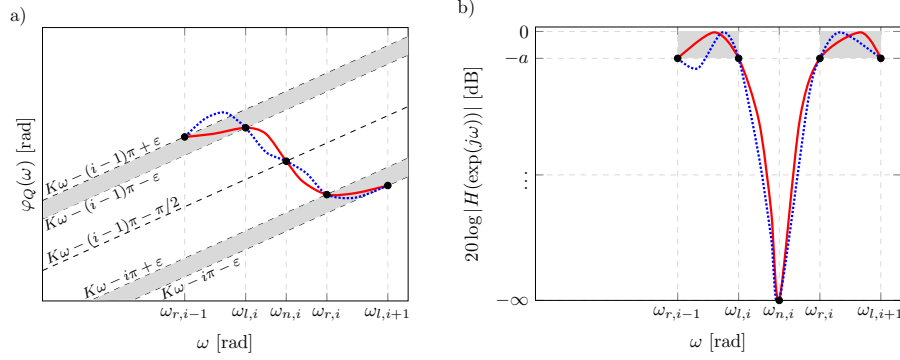


Fig. 1 Graphical interpretation of specifications of IIR multiple-notch filter with symmetric magnitude responses about notch frequencies

shaded regions (for $\omega \in \mathcal{P}_i \cup \mathcal{P}_{i+1}$) and defined points, red solid line in Fig. 1a), all specifications are met, Fig. 1b). The case when $\varphi_Q(\omega)$ passes through defined points but not shaded region for $\omega \in \mathcal{P}_i$, indicated by blue dotted line in Fig. 1a), results in specifications violation in i -th pass-band, Fig. 1b).

2.2 Determination of the all-pass filter coefficients

Once specifications of the multiple-notch filter are transformed to those of an equivalent all-pass filter, it is necessary to establish a mathematical relationship between coefficients and the phase response of the all-pass filter. Since proposed method, introduced later, assumes suitable decomposition of the all-pass filter transfer function $Q_N(z)$, i.e. unknown coefficients q_i , for $i = 1, 2, \dots, N$, are determined indirectly, following discussion relates to all-pass filters in general. Derived conclusions will be used in proposed algorithm.

Let $P_L(z)$ denotes the transfer function of the L -th order all-pass filter:

$$P_L(z) = z^{-L} \left(1 + \sum_{i=1}^L p_i z^i \right) \left(1 + \sum_{i=1}^L p_i z^{-i} \right)^{-1} \quad (11)$$

Determination of coefficients p_i , for $i = 1, 2, \dots, L$, is based on relation [6]:

$$\begin{aligned} \sum_{i=1}^L p_i \{ \cos[\phi_P(\omega) + L\omega - i\omega] + \sin[\phi_P(\omega) + L\omega - i\omega] - \cos i\omega - \sin i\omega \} \\ = 1 - \cos[\phi_P(\omega) + L\omega] - \sin[\phi_P(\omega) + L\omega] \end{aligned} \quad (12)$$

where $\phi_P(\omega)$ is a phase response of the all-pass filter $P_N(z)$. By employing

$$\varphi_P(\omega) = \frac{\phi_P(\omega) + L\omega}{2} = -\arg \left\{ 1 + \sum_{i=1}^L p_i z^{-i} \right\}_{z=\exp(j\omega)} \quad (13)$$

in (12) and after a few simple trigonometric manipulations, equation (12) can be rewritten as:

$$\sum_{i=1}^L p_i \sin[\varphi_P(\omega) - i\omega] = -\sin \varphi_P(\omega) \quad (14)$$

Under the assumption that transfer function $P_L(z)$ has only simple poles (i.e. poles of order 1), unknown coefficients vector $\mathbf{p} = [p_1 \ p_2 \ \dots \ p_L]^T$ can be determined by solving a system of linear equations if $M \geq L$ pairs $\{(\omega_m, \varphi_P(\omega_m)) \mid m = 1, 2, \dots, M\}$ are known. A unique solution for \mathbf{p} exists if $M = L$ and the system of equations is well-defined, while for $M > L$ obtained system of linear equations is overdetermined and has only approximate solution [22, 23].

3 The proposed method

The order of the all-pass filter characterizing multiple-notch filter in methods [4–6] is equal to double the number of notch frequencies, i.e. $N = 2K$, which leads to a nearly constant phase response of the all-pass filter in pass-bands. However, obtained multiple-notch filter may not meet all specifications, while the magnitude response is asymmetrical about notch frequencies. Therefore, an iterative algorithm is proposed, by which the order N of the all-pass filter $Q_N(z)$ and coefficients' vector $\mathbf{q} = [q_1 \ q_2 \ \dots \ q_N]^T$ can be determined, so that specifications given by (6) and (7) are exactly met. This can be achieved only if the order of the all-pass filter $Q_N(z)$ is greater than or equal to triple the number of notch frequencies, i.e. $N \geq 3K$. The proposed algorithm is applicable to both single- and multiple-notch filter design.

Since $3K$ pairs $(\bar{\omega}_m, \varphi_Q(\bar{\omega}_m))$, given by (10), are provided by specifications, system of linear equations constructed by utilizing equations (10) and (14), for $N = 3K$ has the unique solution for \mathbf{q} , given by:

$$\mathbf{q} = \mathbf{G}^{-1} \mathbf{t} \quad (15)$$

where $\mathbf{G} = [g_{m,i}]$ is $3K \times 3K$ square matrix, while $\mathbf{t} = [t_1 \ t_2 \ \dots \ t_{3K}]^T$ is a $3K \times 1$ column vector such that:

$$g_{m,i} = \sin[\varphi_Q(\bar{\omega}_m) - i\bar{\omega}_m], \quad t_m = -\sin \varphi_Q(\bar{\omega}_m) \quad (16)$$

Obtained $\varphi_Q(\omega)$, for $N = 3K$, does not necessarily satisfy design constraints given by equation (7). In this case, the order of the all-pass filter has to be greater than $3K$, leading to an underdetermined system of linear equations constructed by using (10), with infinite number of solutions for the unknown vector \mathbf{q} . However, solutions of interest are only those satisfying (7).

Let us consider the following decomposition of the transfer function $Q_N(z)$ of the all-pass filter:

$$Q_N(z) = B_{3K}(z)C_{N-3K}(z) \quad (17)$$

where $B_{3K}(z)$ and $C_{N-3K}(z)$ are transfer functions of two all-pass filters of orders $3K$ and $(N - 3K)$, respectively. Note, if N equals $3K$, one has that $Q_N(z) = B_{3K}(z)$, i.e. $\mathbf{q} = \mathbf{b} = [b_1 \ b_2 \ \dots \ b_{3K}]^T$. Taking into account (13), equation (17) can be rewritten as

$$\varphi_Q(\omega) = \varphi_B(\omega) + \varphi_C(\omega) \quad (18)$$

The idea is to utilize the all-pass filter $B_{3K}(z)$, i.e. its corresponding function $\varphi_B(\omega)$ to set notch, left- and right-hand cutoff frequencies to their prescribed positions (equation (10)), while pass-bands ripple value is being jointly controlled by the all-pass filter $C_{N-3K}(z)$, i.e. its corresponding function $\varphi_C(\omega)$, for $N > 3K$ (equation (7)). Namely, for a fixed value $N > 3K$, main steps in l -th ($l \geq 1$) iteration of the proposed algorithm are:

- update the coefficients vector $\mathbf{c}^{(l)} = [c_1^{(l)} \ c_2^{(l)} \ \dots \ c_{N-3K}^{(l)}]^T$ using previously determined $\mathbf{b}^{(l-1)}$, in such a way that deviation of the pass-bands magnitude response is minimized, which can be performed by utilizing one of many minimization techniques. In this paper, we choose to determine the vector $\mathbf{c}^{(l)}$ as the least-square solution of the overdetermined system of linear equations, constructed by setting the magnitude response of the multiple-notch filter to one at $M > N - 3K$ distinct frequencies in pass-bands:

$$r = 1, 2, \dots, K + 1 :$$

$$\begin{aligned} \tilde{\omega}_{r,i} &= i\Delta\omega + \min \mathcal{P}_r, \\ |H(\exp(j\tilde{\omega}_{r,i}))| &= 1 \Rightarrow \varphi_Q(\tilde{\omega}_{r,i}) = K\tilde{\omega}_{r,i} - (r-1)\pi \quad (19) \\ i &= 1, \dots, m_r = \left\lceil \frac{\max \mathcal{P}_r - \min \mathcal{P}_r}{\Delta\omega} - 1 \right\rceil, \end{aligned}$$

where $M = \sum_{r=1}^{K+1} m_r$, and m_r is the number of equidistant frequencies in the r -th pass-band for $r = 1, 2, \dots, K + 1$.

Based on the previous discussion and using equations (18) and (19), $\mathbf{c}^{(l)}$ should be determined such that:

$$\varphi_C^{(l)}(\tilde{\omega}_{r,i}) = K\tilde{\omega}_{r,i} - (r-1)\pi - \varphi_B^{(l-1)}(\tilde{\omega}_{r,i}), \quad i = 1, 2, \dots, m_r \quad (20)$$

for $r = 1, 2, \dots, K + 1$. System of linear equations constructed by using (14) and (20) has a least-square solution for the coefficients vector $\mathbf{c}^{(l)}$ given by:

$$\mathbf{c}^{(l)} = \begin{bmatrix} \mathbf{W}_1^{(l)} \\ \mathbf{W}_2^{(l)} \\ \vdots \\ \mathbf{W}_{K+1}^{(l)} \end{bmatrix}^\dagger \begin{bmatrix} \mathbf{y}_1^{(l)} \\ \mathbf{y}_2^{(l)} \\ \vdots \\ \mathbf{y}_{K+1}^{(l)} \end{bmatrix} \quad (21)$$

where \dagger is a pseudo-inverse matrix operator, $\mathbf{W}_r^{(l)} = [w_{i,k}^{(l,r)}]$ is a $m_r \times (N - 3K)$ matrix and $\mathbf{y}_r^{(l)} = [y_1^{(l,r)} \ y_2^{(l,r)} \ \dots \ y_{m_r}^{(l,r)}]^T$ is a $m_r \times 1$ column vector such that:

$$w_{i,k}^{(l,r)} = \sin \left[(K - k) \tilde{\omega}_{r,i} - \varphi_B^{(l-1)}(\tilde{\omega}_{r,i}) \right], \quad y_i^{(l,r)} = -\sin \left[K \tilde{\omega}_{r,i} - \varphi_B^{(l-1)}(\tilde{\omega}_{r,i}) \right] \quad (22)$$

- update the coefficients vector $\mathbf{b}^{(l)}$ using $\mathbf{c}^{(l)}$, such that specifications regarding to positions of notch, left- and right-hand cutoff frequencies are satisfied. Using equations (10) and (18), desired $\varphi_B^{(l)}(\bar{\omega}_m)$ for $m = 1, 2, \dots, 3K$, can be determined as

$$\varphi_B^{(l)}(\bar{\omega}_m) = \varphi_Q(\bar{\omega}_m) - \varphi_C^{(l)}(\bar{\omega}_m) \quad (23)$$

System of linear equations, constructed by utilizing equations (14) and (23) has the unique solution for the coefficients vector $\mathbf{b}^{(l)}$ given by:

$$\mathbf{b}^{(l)} = \mathbf{V}^{(l)-1} \mathbf{s}^{(l)} \quad (24)$$

where $\mathbf{V}^{(l)} = [v_{m,i}^{(l)}]$ is a $3K \times 3K$ square matrix, while $\mathbf{s}^{(l)} = [s_1^{(l)} \ s_2^{(l)} \ \dots \ s_{3K}^{(l)}]^T$ is a $3K \times 1$ column vector such that:

$$v_{m,i}^{(l)} = \sin \left[\varphi_Q(\bar{\omega}_m) - \varphi_C^{(l)}(\bar{\omega}_m) - i \bar{\omega}_m \right], \quad s_m^{(l)} = -\sin \left[\varphi_Q(\bar{\omega}_m) - \varphi_C^{(l)}(\bar{\omega}_m) \right] \quad (25)$$

for $m = 1, 2, \dots, 3K$.

Mentioned steps are repeated until either all specifications are met or maximum value (in all pass-bands) of the left side of the inequality (7) cannot be further minimized. In the latter case, order of the all-pass filter has to be increased. Pseudo-code for the proposed IIR multiple-notch filter design procedure is given in Algorithm 1.

Algorithm 1: Proposed iterative algorithm for the IIR multiple-notch filter design

```

Initialize:  $l = 0$ ;
 $N = 3K$ ;
Determine  $\mathbf{q}^{(0)} = \mathbf{b}^{(0)}$  using (15);
temp =  $\max_{\substack{\omega \in \mathcal{P}_i \\ 1 \leq i \leq K+1}} |\varphi_Q^{(0)}(\omega) - K\omega + (i-1)\pi|$ ;
if temp >  $\varepsilon$  then
   $N = N + 1$ ;
   $\varepsilon_{\max} = (N + 1)\pi$ ;
  while  $\varepsilon_{\max} > \varepsilon$  do
     $l = l + 1$ ;
    Determine  $\mathbf{c}^{(l)}$  using (21);
    Determine  $\mathbf{b}^{(l)}$  using (24);
    temp =  $\max_{\substack{\omega \in \mathcal{P}_i \\ 1 \leq i \leq K+1}} |\varphi_Q^{(l)}(\omega) - K\omega + (i-1)\pi|$ ;
    if temp <  $\alpha \cdot \varepsilon_{\max}$  then
       $\varepsilon_{\max} = \text{temp}$ ;
    else
       $N = N + 1$ ;
       $\varepsilon_{\max} = (N + 1)\pi$ ;
    end
  end
   $\mathbf{b} = \mathbf{b}^{(l)}$ ;
   $\mathbf{c} = \mathbf{c}^{(l)}$ ;
else
   $\mathbf{b} = \mathbf{b}^{(0)}$ ;
   $\mathbf{c} = [ ]$ ;
end

```

Note, for $N > 3K$, if either of the unknown coefficients vectors \mathbf{b} and \mathbf{c} is fixed, then the solution to the other one has a closed-form.

Convergence factor α , whose value is close to one, ensures that algorithm converges more rapidly. However, its value should be chosen with great concern. If the chosen value is too low, the order of the obtained all-pass filter (hence, multiple-notch filter) will be increased unnecessarily. On the other side, if the chosen value is too close to one, number of iterations will increase. According to many runs of proposed algorithm for various examples, it was adopted that optimal convergence factor value equaled 0.985. This value corresponds to the relative error $(\text{temp} - \varepsilon_{\max}) / \varepsilon_{\max}$ equal to -1.5% .

3.1 Convergence speed

The proposed algorithm is applicable to both single- and multiple-notch filter design. In case of the single-notch filter design, the order of the corresponding all-pass filter equals 3, i.e. its coefficients are determined in iteration zero, for $\omega_n \in [0.1\pi, 0.9\pi]$ rad, $a \in [0.15, 3]$ dB and $\text{BW} \in [0.004\pi, 0.1\pi]$ rad (which can be proved numerically).

On the other side, the order and the coefficients of the all-pass filter characterizing the multiple-notch filter, are obtained in a small number of iterations – if they

are not obtained in the iteration zero. To support this claim, a series of algorithm runs was performed for various notch-bandwidths and pass-band ripple values, and for two minimum values of pass-band widths between notch frequencies (0.05π and 0.075π), assuming $\alpha = 0.985$, $\Delta\omega = \pi/20$ as well as notch frequencies from a finite set of frequencies $\Omega_N = \{0.1\pi, 0.125\pi, 0.15\pi, \dots, 0.9\pi\}$. Obtained maximum number of iterations (worst-case) are given in Tab. 1 for the cases when number of notch frequencies K equals to 2, 3 and 4.

Table 1 The maximum number of iterations needed for algorithm to converge for various notch-bandwidths and pass-band ripple values, $\omega_{n,i} \in \Omega_N, i = 1, 2, \dots, K$, and $K = 2, 3, 4$. Minimum value of pass-band widths between notch frequencies is greater than or equal to 0.05π (0.075π).

$$\min_{2 \leq i \leq K} \{\max \mathcal{P}_i - \min \mathcal{P}_i\} \geq 0.05\pi \text{ (} 0.075\pi \text{)}$$

$K = 2$		BW/ π [rad]					
		0.004	0.008	0.01	0.05	0.075	0.10
a [dB]	0.15	1 (0)	1 (0)	2 (1)	4 (2)	3 (2)	3 (1)
	0.72	1 (0)	1 (0)	1 (1)	3 (1)	3 (1)	3 (1)
	1.29	1 (0)	1 (0)	1 (1)	4 (1)	3 (1)	1 (1)
	1.86	0 (0)	1 (0)	1 (0)	4 (1)	1 (1)	1 (1)
	2.43	0 (0)	1 (0)	1 (0)	4 (1)	1 (1)	1 (1)
	3.00	0 (0)	1 (0)	1 (0)	4 (1)	1 (1)	1 (0)

$K = 3$		BW/ π [rad]					
		0.004	0.008	0.01	0.05	0.075	0.10
a [dB]	0.15	7 (7)	8 (8)	8 (7)	18 (8)	17 (7)	12 (4)
	0.72	6 (6)	13 (7)	13 (6)	9 (6)	8 (5)	5 (0)
	1.29	5 (4)	13 (5)	12 (6)	8 (5)	6 (5)	3 (0)
	1.86	6 (4)	10 (5)	10 (5)	9 (5)	6 (3)	2 (0)
	2.43	6 (2)	10 (4)	10 (5)	10 (3)	6 (1)	2 (0)
	3.00	6 (5)	10 (4)	11 (4)	8 (3)	4 (1)	2 (0)

$K = 4$		BW/ π [rad]					
		0.004	0.008	0.01	0.05	0.075	0.10
a [dB]	0.15	7 (2)	16 (2)	21 (2)	19 (6)	19 (2)	2 (0)
	0.72	5 (1)	11 (1)	13 (4)	14 (4)	6 (1)	1 (0)
	1.29	5 (1)	13 (1)	16 (5)	10 (5)	5 (1)	1 (0)
	1.86	6 (1)	13 (1)	12 (5)	10 (1)	5 (1)	1 (0)
	2.43	9 (1)	10 (5)	14 (4)	9 (1)	2 (1)	1 (0)
	3.00	12 (1)	22 (1)	17 (1)	9 (1)	2 (0)	1 (0)

When pass-band widths between notch frequencies are greater than or equal to 0.075π rad, the order and coefficients of the all-pass filter are obtained in less than 10 iterations. Maximum number of iterations (worst-case) slightly increases if the minimum pass-band width is set to be equal to 0.05π rad, partially due to increased order of the obtained all-pass filter, but primarily due to adopted convergence factor value. However, choosing lower value of convergence factor α will decrease worst-

case number of iterations in some, but increase in other cases. The latter will result in unnecessary increase of obtained all-pass filter order.

3.2 The dependence of the all-pass filter $Q_N(z)$ order and the maximum pole radius on the pass-bands ripple value and notch bandwidths

There is no exact mathematical relationship between the order of the all-pass filter $Q_N(z)$ and magnitude response specifications of the multiple-notch filter. A lower value for N is highly desirable, among other things due to a lower group-delay in pass-bands. Furthermore, hardware realization complexity increases if the filter has poles close to the unit circle, due to high sensitivity to coefficient quantization errors.

The orders of the all-pass filter $Q_N(z)$ and maximum pole radii ρ_{\max} for $K = 2$, $\omega_{n,1} = 0.25\pi$, $\omega_{n,2} = 0.375\pi$, $BW = BW_1 = BW_2 \in [0.004\pi, 0.12\pi]$ and $a \in [0.15, 3]$ dB, obtained by the proposed algorithm, are illustrated in Fig. 2a) and Fig. 2b), respectively. Number of iterations for algorithm to converge is given in Fig. 2c). As can

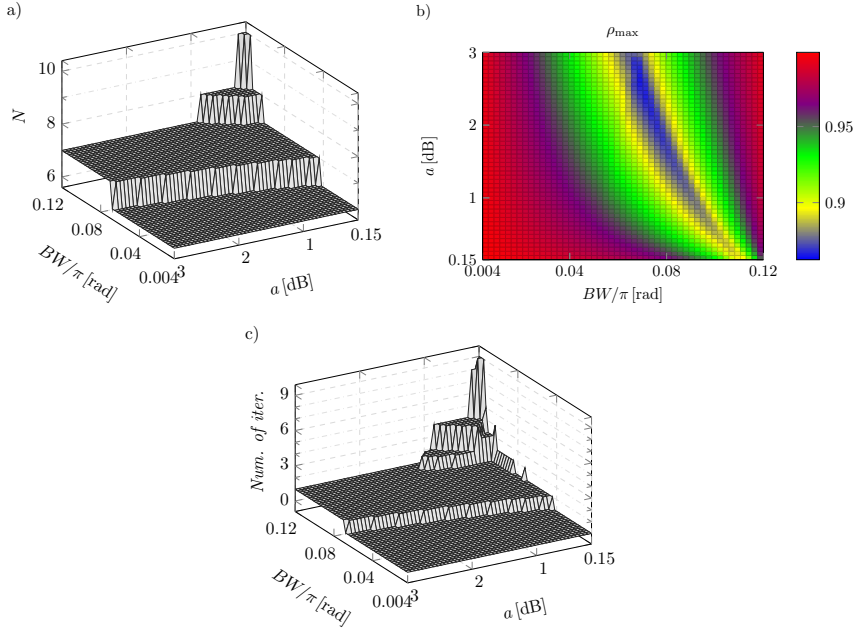


Fig. 2 $\omega_{n,1} = 0.25\pi$, $\omega_{n,2} = 0.375\pi$. a) The order N of the all-pass filter $Q_N(z)$. b) Maximum pole radius ρ_{\max} . c) Number of iterations for algorithm to converge.

be observed in Fig. 2a), for small enough values of notch bandwidths ($BW < 0.04\pi$), the order N of the all-pass filter $Q_N(z)$ equals triple the number of notch frequencies, for all $a \in [0.15, 3]$ dB; however, hardware complexity is expected to be high, since the maximum pole radius is very close to one, which is particularly true if a is less, Fig. 2b). On the other side, if BW is higher, N increases and correspondingly

the number of iterations required for algorithm to converge. In the limiting case, i.e. when BW approaches its upper boundary value (width of the pass-band between notch frequencies, $\omega_{n,2} - \omega_{n,1} - \text{BW}$, approaches $0.005\pi \approx 0$) and a approaches its lower boundary value, the order N of the all-pass filter $Q_N(z)$ has its maximum, as well as the number of iterations, Fig. 2c).

For a fixed value of a , with BW increasing from its lower boundary value, the maximum pole radius decreases from its maximum (red color in Fig. 2b)) to its minimum value (blue/green or yellow color, depending on the pass-bands ripple value a), after which it starts to increase. This suggests that in some cases even stronger specifications can be met, with decreasing maximum pole radius ρ_{\max} and/or order N at the same time. For example, if specifications are such that $\text{BW} = 0.08\pi$ and $a = 3$ dB, one obtains that $N = 7$ and $\rho_{\max} = 0.9157$. However, if BW is set to 0.06π , keeping a unchanged, obtained N and ρ_{\max} are equal to 6 and 0.8839, respectively. This means that both order and maximum pole radius decrease. On the other side, if $\text{BW} = 0.07\pi$ and $a = 1.75$ dB, only maximum pole radius decreases (0.8912), while the order N remains at 7.

Similar conclusions can be drawn for the multiple-notch filter with any number of and arbitrary position of notch frequencies, which was verified through many runs of the proposed algorithm.

4 Sensitivity considerations

Generally speaking, once multiple-notch filter coefficients are determined, it can be realized using one of several equivalent filter structures. If IIR multiple-notch filter is realized by parallel connection of delay line and all-pass filter $Q_N(z)$, a relative sensitivity of the filter magnitude response to changes of multiplier coefficients d_j is not useful for comparing different structures, since division by zero (infinitely high attenuation at notch frequencies) is not possible:

$$S_{d_j}^{|H|}(\omega) = \frac{d_j}{|H(\exp(j\omega))|} \frac{\partial}{\partial d_j} |H(\exp(j\omega))| \quad (26)$$

Hence, semirelative sensitivity of the magnitude response to changes of multiplier coefficients d_j will be used:

$$\tilde{S}_{d_j}^{|H|}(\omega) = d_j \frac{\partial}{\partial d_j} |H(\exp(j\omega))| \quad (27)$$

along with corresponding worst-case semirelative sensitivity function:

$$\text{WS}^{|H|}(\omega) = \sum_j \left| \tilde{S}_{d_j}^{|H|}(\omega) \right| \quad (28)$$

Furthermore, if all-pass filter $Q_N(z)$ is realized by cascading first- and second-order all-pass sections, which leads to a significant reduction of overall sensitivity [17–19, 21]:

$$\varphi_Q(\omega) = \sum_i \varphi_{Q_i}(\omega), \quad (29)$$

and employing (5), equations (27) and (28) can be rewritten as:

$$\tilde{S}_{d_j}^{|H|}(\omega) = -\text{sgn}(\cos(\varphi_Q(\omega) - K\omega)) \sin(\varphi_Q(\omega) - K\omega) \tilde{S}_{d_j}^{\varphi_Q}(\omega) \quad (30)$$

$$\text{WS}^{|H|}(\omega) = \left| \sin(\varphi_Q(\omega) - K\omega) \left| \sum_i \sum_j \tilde{S}_{d_j}^{\varphi_{Q_i}}(\omega) \right| \right| \quad (31)$$

where:

$$\tilde{S}_{d_j}^{\varphi_Q}(\omega) = d_j \frac{\partial}{\partial d_j} \varphi_Q(\omega), \quad \tilde{S}_{d_j}^{\varphi_{Q_i}}(\omega) = d_j \frac{\partial}{\partial d_j} \varphi_{Q_i}(\omega) \quad (32)$$

denote semirelative sensitivities of $\varphi_Q(\omega)$ and $\varphi_{Q_i}(\omega)$ to the change of the multiplier coefficient d_j .

It is evident, from (31), that the worst-case sensitivity of multiple-notch filter magnitude response can be reduced by selecting realization structures for each first- and second-order sections which have low semirelative sensitivities $\tilde{S}_{d_j}^{\varphi_{Q_i}}(\omega)$ [17–19, 21]. After the adoption of suitable realization structures taking into account sections given in [17–19, 21] and if fixed-point implementation is considered, fractional part lengths for every multiplier coefficient d_j can be determined in order to keep performances of the multiple-notch filter as close as possible to desired. Namely, if relative change in values of all multiplier coefficients is less than:

$$\delta = \frac{10^{-a_{notch}/20}}{\max_{1 \leq k \leq K} \text{WS}^{|H|}(\omega_{n,k})}, \quad (33)$$

the attenuation in dB at notch frequencies $\omega_{n,k}$, $k = 1, \dots, K$, will be greater than or equal to the prescribed value a_{notch} . A more precise determination of fractional part lengths for coefficients involves consideration of the individual semirelative sensitivity functions $\tilde{S}_{d_j}^{\varphi_{Q_i}}(\omega)$ and their contribution to the worst-case semirelative sensitivity, which leads to adoption of different values for the relative change of each multiplier coefficient.

5 Design examples

The efficiency of the proposed algorithm will be verified by designing two multiple-notch filters. In both examples, $\Delta\omega$ was assumed to have the value of $\pi/20$, Eq. (19), while convergence factor α equals 1.

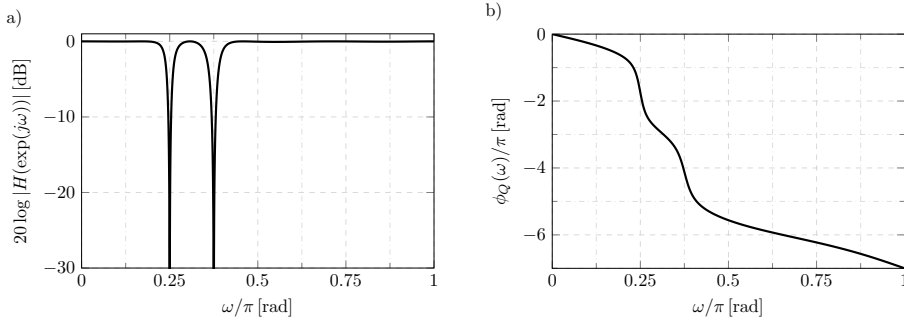
Example 1: Specifications of the multiple notch filter with $K = 2$ are: $\omega_{n,1} = 0.25\pi$, $\omega_{n,2} = 0.375\pi$, $\text{BW}_1 = 0.08\pi$, $\text{BW}_2 = 0.1\pi$, $a = 0.15$ dB.

Given specifications are met for $N = 7$ (after 2 iterations), and obtained filter has poles whose radiuses ρ , and phase angles θ are given in Tab. 2. Last two columns contain names of first- and second-order all-pass sections and their transfer functions which correspond to the lowest sensitivity realization structures. These sections were chosen among many given in [17–19, 21].

Table 2 Example 1. Radiuses and phase angles of multiple-notch filter poles

ρ	θ/π [rad]	Section	Transfer function
0.961453308136	± 0.249527181294	ST2A	$\frac{1 - 2d_1 - 2(1 - d_1)(1 - 2d_2)z^{-1} + z^{-2}}{1 - 2(1 - d_1)(1 - 2d_2)z^{-1} + (1 - 2d_1)z^{-2}}$
0.943391899363	± 0.375804659065	KW2A	$\frac{1 + d_3 - d_4 - (d_3 + d_4)z^{-1} + z^{-2}}{1 - (d_3 + d_4)z^{-1} + (1 + d_3 - d_4)z^{-2}}$
0.603534059283	± 0.333473298081	MH2A	$\frac{d_5d_6 - d_5z^{-1} + z^{-2}}{1 - d_5z^{-1} + d_5d_6z^{-2}}$
0.488058692602	1	MH1	$\frac{-d_7 + z^{-1}}{1 - d_7z^{-1}}$

The magnitude response of a multiple-notch filter in dB and the phase response of the all-pass filter $Q_N(z)$ are illustrated in Fig. 3a) and Fig. 3b). Worst-case semirelative sensitivity of multiple-notch filter magnitude response and semirelative sensitivities of magnitude response to changes of multiplier coefficients d_j , $j = 1, 2, \dots, 7$, are shown in Fig. 4a) and Fig. 4b). As can be seen in Fig. 4, magnitude response

**Fig. 3** Example 1. a) The magnitude response of the multiple-notch filter in dB. b) The phase response of the all-pass filter $Q_N(z)$

is most sensitive in stop-bands, and to relative changes of multiplier coefficients d_2 and d_4 , that correspond to sections whose poles are close to the unit circle. Since $\max \left\{ \text{WS}^{|H|}(\omega_{n,1}), \text{WS}^{|H|}(\omega_{n,2}) \right\} = 12.4643$, a relative change in coefficients values should be less than 0.45% (33), if the attenuation at notch frequencies is desired to be at least 25 dB. If the fixed-point implementation is considered, fractional part lengths for multiplier coefficients d_1, d_2, \dots, d_7 are equal to 13, 11, 9, 9, 7, 7 and 9 bits, respectively. Simulation in the limited word-length environment gives values of the magnitude response at frequencies $\bar{\omega}_m$, $m = 1, 2, \dots, 6$, as follows: 0.1542 dB, 36.0675 dB, 0.1475 dB, 0.1444 dB, 30.3726 dB and 0.1548 dB.

Example 2: Specifications of the multiple notch filter with $K = 3$ are: $\omega_{n,1} = 0.2\pi$, $\omega_{n,2} = 0.4\pi$, $\omega_{n,3} = 0.8\pi$, $\text{BW}_1 = 0.06\pi$, $\text{BW}_2 = 0.1\pi$, $\text{BW}_3 = 0.075\pi$, $a = 1$ dB.

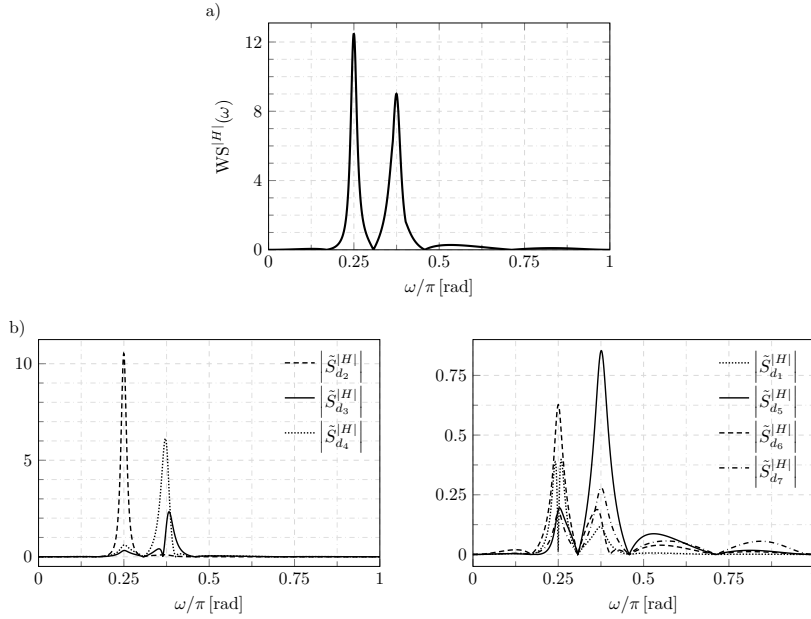


Fig. 4 Example 1. a) The worst-case semirelative sensitivity of the magnitude response. b) Semirelative sensitivities of the magnitude response to changes of multiplier coefficients d_j , $j = 1, 2, \dots, 7$

In this case, given specifications are met for $N = 9$, which is the lowest value for the order of the all-pass filter $Q_N(z)$ that can be obtained by the algorithm. The magnitude response of the multiple-notch filter in dB and the phase response of the all-pass filter $Q_N(z)$ are given in Fig. 5a) and Fig. 5b). IIR multiple-notch filter poles

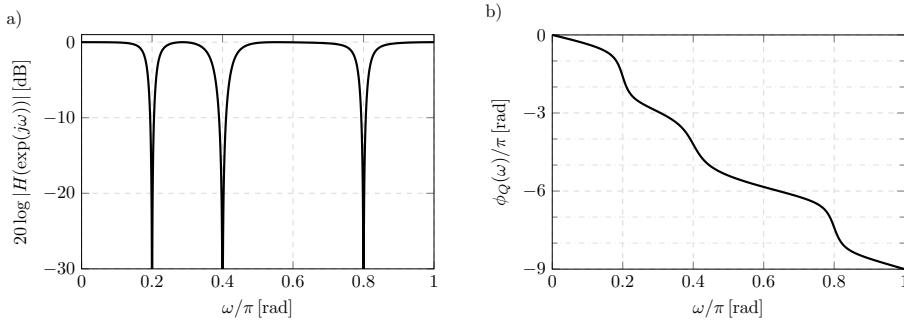


Fig. 5 Example 2. a) The magnitude response of the multiple-notch filter in dB. b) The phase response of the all-pass filter $Q_N(z)$

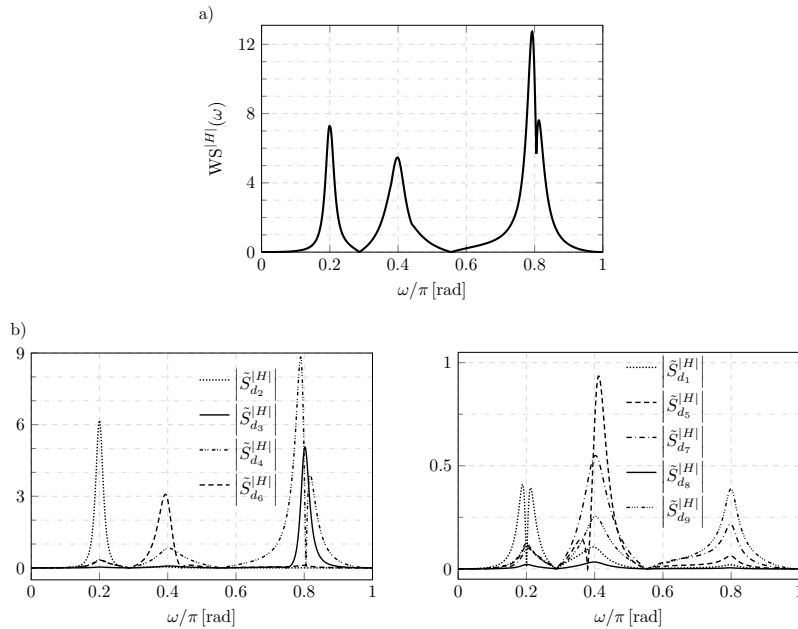
in terms of radiuses ρ and phase angles θ are given in Tab. 3.

As in the previous example, sections that exhibit the lowest sensitivity (for each pole location) were chosen from those given in [17–19,21], and the worst-case semirelative sensitivity of the multiple-notch filters magnitude response and semirel-

Table 3 Example 2. Radiuses and phase angles of multiple-notch filter poles

ρ	θ/π [rad]	Section	Transfer function
0.948472209582	± 0.199828022531	ST2A	$\frac{1 - 2d_1 - 2(1 - d_1)(1 - 2d_2)z^{-1} + z^{-2}}{1 - 2(1 - d_1)(1 - 2d_2)z^{-1} + (1 - 2d_1)z^{-2}}$
0.941360544561	± 0.799950705486	KW2B	$\frac{d_3 + d_4 - 1 - (d_3 - d_4)z^{-1} + z^{-2}}{1 - (d_3 - d_4)z^{-1} + (d_3 + d_4 - 1)z^{-2}}$
0.904353710814	± 0.400541701653	KW2A	$\frac{1 + d_5 - d_6 - (d_5 + d_6)z^{-1} + z^{-2}}{1 - (d_5 + d_6)z^{-1} + (1 + d_5 - d_6)z^{-2}}$
0.476010759000	± 0.351330174875	IS	$\frac{d_7 + (-d_8 - 2d_7 + d_7d_8)z^{-1} + z^{-2}}{1 + (-d_8 - 2d_7 + d_7d_8)z^{-1} + d_7z^{-2}}$
0.360632453554	1	MH1	$\frac{-d_9 + z^{-1}}{1 - d_9z^{-1}}$

ative sensitivities of the magnitude response to changes in multiplier coefficients d_j , $j = 1, 2, \dots, 9$, were calculated, Fig. 6.

**Fig. 6** Example 2. a) The worst-case semirelative sensitivity of the magnitude response. b) Semirelative sensitivities of the magnitude response to changes of multiplier coefficients d_j , $j = 1, 2, \dots, 9$

The magnitude response of the multiple-notch filter is most sensitive about notch, left- and right-hand cutoff frequencies, which leads them to drift from their specified positions. However, from the determined worst-case semirelative sensitivity of the magnitude response function, using (33), if the attenuation at notch frequencies is desired to be at least 30 dB, the relative change in coefficients values should be less than 0.32%. This corresponds to 12, 9, 11, 6, 10, 10, 7, 13 and 10 bits, needed for

fractional parts of multiplier coefficients d_1, d_2, \dots, d_9 , respectively, if fixed-point implementation is considered. Simulation in the limited word-length environment has verified the design accuracy, since following values of the magnitude response at frequencies $\bar{\omega}_m$ ($m = 1, 2, \dots, 9$) were obtained: 1.0078 dB, 38.0572 dB, 0.9813 dB, 0.9902 dB, 43.0531 dB, 0.9977 dB, 1.0285 dB, 42.1863 dB and 1.0346 dB.

6 Comparison to existing methods

Not all of all-pass based IIR digital multiple-notch filter design methods [4–7] can be generalized to a case of an arbitrary attenuation value (i.e. pass-bands ripple value) at cutoff frequencies. As mentioned, *Method I* given in [6] is the same method presented in [4, 5] with overcame limitations regarding to tangent operations. Furthermore, neither one of those methods guarantees that specifications are exactly met.

However, for the sake of comparison, two methods guaranteeing that specifications regarding notch frequencies positions are exactly met were chosen: *Method I* (specifications regarding positions of notch and left-hand cutoff frequencies are met) and *Method II* (specifications regarding positions of notch and right-hand cutoff frequencies are met) given in [6].

While $2K$ unknown coefficients of multiple-notch filters designed by *Methods I* and *II* [6] are determined by solving the system of $2K$ linear equations, proposed design method requires solving a system of $3K$ equations with $3K$ unknown variables in every iteration, and a system of M equations with $(N - 3K)$ unknown variables in the least-square sense in every but the zeroth iteration. Hence, computational complexity of the proposed method is higher than for *Methods I* and *II* [6].

Magnitude responses of multiple-notch filters from examples 1 and 2, obtained by utilizing these two methods as well as the proposed one, are presented in Fig. 7. As

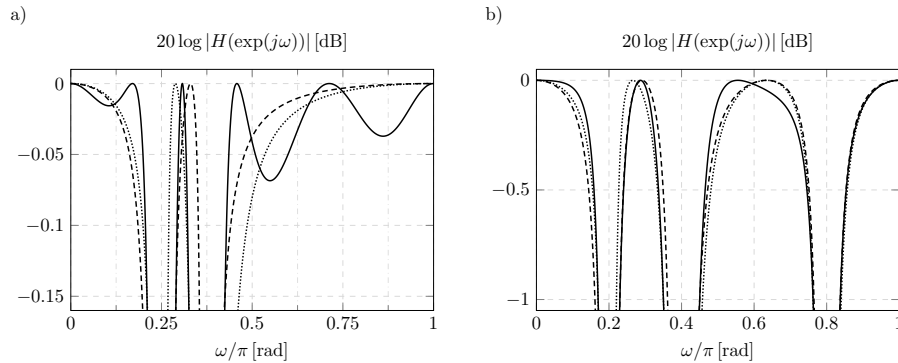


Fig. 7 Magnitude responses in dB obtained by proposed (solid line) and *Methods I* and *II* from [6] (dotted and dashed line, respectively) of the multiple-notch filter from a) Example 1 and b) Example 2

expected, there is a clear drift of left- (*Method I* – dotted line) and right-hand (*Method II* – dashed line) cutoff frequencies from their specified positions. As a result, some of obtained notch bandwidths are narrower, which is more noticeable in case of the filter

from example 1, Fig. 7a), while some of them are wider than specified. Responses of filters from both examples to the sum of sinusoidal interferences

$$x[n] = \sum_{k=1}^K \frac{k}{10} \sin \left(n \cdot \omega_{n,k} + k \cdot \frac{\pi}{3} \right) \quad (34)$$

are given in Fig. 8. As expected, duration of transient response of the filter from ex-

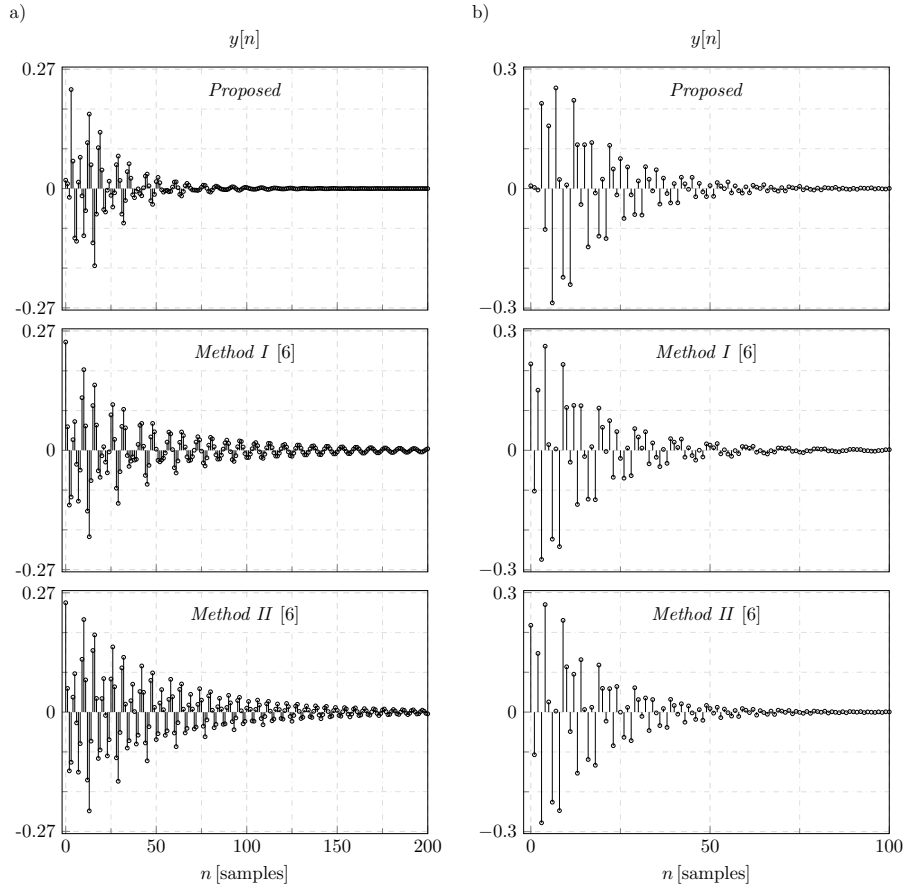


Fig. 8 Responses to sum of sinusoidal interferences, Eq. (34), obtained by proposed and *Methods I* and *II* from [6] of the multiple-notch filter from a) Example 1, b) Example 2

ample 1 designed by proposed method is shorter compared to those of filters designed by considered methods from [6], Fig. 8a). In case of the filter from example 2, since obtained bandwidths when utilizing *Methods I* and *II* are close to those specified, Fig. 7b), durations of transient responses are comparable, Fig. 8b).

Multiple-notch filters designed using proposed algorithm gives higher group-delay value in pass-bands, Fig. 9, compared to those designed by using *Methods I*

and *II* [6], due to a higher order of the all-pass filter characterizing multiple-notch filter in the proposed design.

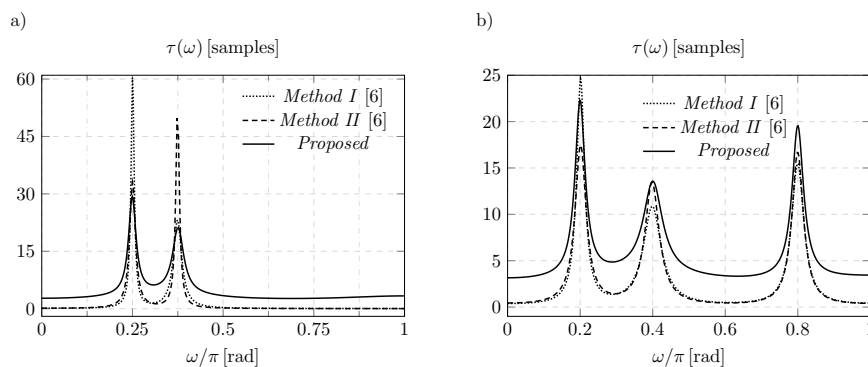


Fig. 9 Group-delays obtained by proposed, *Methods I* and *II* from [6] of the multiple-notch filter from a) Example 1, b) Example 2

Phase responses of all-pass filters from examples 1 and 2, obtained by using the proposed as well as *Methods I* and *II* [6] are given in Fig. 10. While phase responses obtained by *Methods I* and *II* approximate $-2(i-1)\pi$ (constant function), phase responses obtained by proposed method approximate $-2(i-1)\pi - \omega(N-2K)$ (linear function of frequency) in i -th pass-band, for $i = 1, 2, \dots, K+1$.

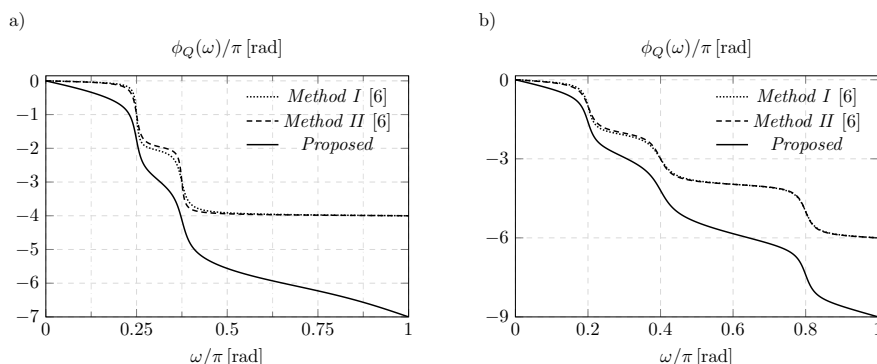


Fig. 10 Phase responses obtained by proposed, *Methods I* and *II* from [6] of the all-pass filter $Q_N(z)$ from a) Example 1, b) Example 2

7 Conclusion

In this paper, novel all-pass based IIR digital multiple-notch filter design method is presented. Although iterative in its nature, the order and coefficients of the all-pass

filter characterizing the desired multiple-notch (or single-notch) filter can be obtained in a small number of iterations. Resulting filter exactly meets all specifications, i.e. its magnitude response is symmetrical about notch frequencies. The order of the all-pass filter characterizing multiple-notch filter is always greater than or equal to triple the number of notch frequencies, which is higher compared to existing all-pass based design methods; however, these methods can not guarantee that specifications of the multiple-notch filter are exactly met. Multiple-notch filter with approximately linear phase characteristic in pass-bands can be obtained if the pass-bands ripple value is decreased. If notch bandwidths are narrow, the order of the obtained all-pass filter, in this case, usually equals triple the number of notch frequencies.

References

1. D. Borio, L. Camoriano, and L. L. Presti, "Two-Pole and Multi-Pole Notch Filters: A Computationally Effective Solution for GNSS Interference Detection and Mitigation," *IEEE Systems Journal*, vol. 2, no. 1, pp. 38–47, March 2008.
2. K. Song and Q. Xue, "Asymmetric dual-line coupling structure for multiple-notch implementation in UWB bandpass filters," *Electronics Letters*, vol. 46, no. 20, pp. 1388–1390, September 2010.
3. Y. D. Jou, Z. P. Lin, and F. K. Chen, "Interference elimination of electrocardiogram signals using IIR multiple notch filters," in *2016 IEEE 5th Global Conference on Consumer Electronics*, pp. 1–2, Oct 2016.
4. S. C. Pei and C. C. Tseng, "IIR multiple notch filter design based on allpass filter," in *TENCON '96. Proceedings., 1996 IEEE TENCON. Digital Signal Processing Applications*, vol. 1, pp. 267–272, Nov 1996.
5. ———, "IIR multiple notch filter design based on allpass filter," *IEEE Transactions on Circuits and Systems II: Analog and Digital Signal Processing*, vol. 44, no. 2, pp. 133–136, 1997.
6. Q. Wang and D. Kundur, "A generalized design framework for IIR digital multiple notch filters," *EURASIP Journal on Advances in Signal Processing*, vol. 2015, no. 1, p. 1, 2015.
7. A. Thamrongmas and C. Charoenlarnopparut, "All-pass based IIR multiple notch filter design using Gröbner Basis," in *Multidimensional (nD) Systems (nDs), 2011 7th International Workshop on*. IEEE, pp. 1–6, 2011.
8. C. C. Tseng and S. C. Pei, "Stable IIR notch filter design with optimal pole placement," *IEEE Transactions on Signal Processing*, vol. 49, no. 11, pp. 2673–2681, Nov 2001.
9. A. Thamrongmas, C. Charoenlarnopparut, and P. Prempre, "A novel design of IIR multiple notch filter based on an all-pass filter by using a pole-reposition technique," *SCIENCEASIA*, vol. 40, no. 5, pp. 362–370, 2014.
10. G. Stančić and S. Nikolić, "Digital linear phase notch filter design based on IIR all-pass filter application," *Digital Signal Processing: A Review Journal*, vol. 23, no. 3, pp. 1065–1069, 2013.
11. S. Nikolić and G. Stančić, "Design of IIR Notch Filter with Approximately Linear Phase," *Circuits, Systems, and Signal Processing*, vol. 31, no. 6, pp. 2119–2131, 2012. [Online]. Available: <http://dx.doi.org/10.1007/s00034-012-9426-x>
12. Y. Jiang, C. Shen, and J. Dai, "A unified approach to the design of IIR and FIR notch filters," in *2016 IEEE International Conference on Acoustics, Speech and Signal Processing (ICASSP)*, pp. 4791–4795, March 2016.
13. Q. Wang, J. Song, and H. Yuan, "Digital Multiple Notch Filter Design Based on Genetic Algorithm," in *2014 Fourth International Conference on Instrumentation and Measurement, Computer, Communication and Control*, pp. 180–183, Sept 2014.
14. C. Duarte, K. E. Barner, and K. Goossen, "Design of IIR Multi-Notch Filters Based on Polynomially-Represented Squared Frequency Response," *IEEE Transactions on Signal Processing*, vol. 64, no. 10, pp. 2613–2623, May 2016.
15. X.-L. Wang, Y.-J. Ge, J.-J. Zhang, and Q.-J. Song, "Discussion on the -3 dB rejection bandwidth of IIR notch filters," in *6th International Conference on Signal Processing, 2002.*, vol. 1, Aug 2002, pp. 151–154 vol.1.

16. L. Tan, J. Jiang, and L. Wang, "Pole-radius-varying IIR notch filter with transient suppression," *IEEE Transactions on Instrumentation and Measurement*, vol. 61, no. 6, pp. 1684–1691, 2012.
17. G. Stoyanov, K. Nikolova, and M. Kawamata, "Low-Sensitivity Design of Allpass Based Fractional Delay Digital Filters," in *Digital Filters*, Prof. Fausto Pedro García Márquez, Ed. InTech, 2011, ch. 7. [Online]. Available: <http://www.intechopen.com/books/digital-filters/low-sensitivity-design-of-allpass-based-fractional-delay-digital-filters>
18. G. Stoyanov, Z. Nikolova, K. Ivanova, and V. Anzova, "Design and realization of efficient IIR digital filter structures based on sensitivity minimizations," in *2007 8th International Conference on Telecommunications in Modern Satellite, Cable and Broadcasting Services*, pp. 299–308, Sept 2007.
19. K. Nikolova, G. Stoyanov, and M. Kawamata, "Low-sensitivity design and implementation of allpass based fractional delay digital filters," in *2009 European Conference on Circuit Theory and Design*, pp. 603–606, Aug 2009.
20. G. Jovanovic-Dolecek and S. K. Mitra, "Symbolic sensitivity analysis of digital filter structures using MATLAB," in *9th International Conference on Electronics, Circuits and Systems*, vol. 3, pp. 903–906, 2002.
21. G. Stoyanov and H. Clausert, "A Comparative Study of First-Order Digital Allpass Filter Sections," *Frequenz*, vol. 48, pp. 221–226, 1994.
22. J. R. Rice, *Numerical methods, software, and analysis*, 2nd ed. Academic Press, 1993.
23. J. A. Cadzow, "Minimum l_1 , l_2 , and l_∞ Norm Approximate Solutions to an Overdetermined System of Linear Equations," *Digital Signal Processing*, vol. 12, no. 4, pp. 524–560, 2002.